Clim. Past Discuss., https://doi.org/10.5194/cp-2017-132
Manuscript under review for journal Clim. Past
Discussion started: 16 October 2017

Climate of the Past Discussions

Simulation of the Greenland Ice sheet over two glacial cycles: Investigating a sub-ice shelf melt parameterisation and relative sea level forcing in an ice sheet-ice shelf model.

Sarah L. Bradley[1,2], Thomas J. Reerink[1], Roderik S.W. van de Wal[1], Michiel M. Helsen[1]

1 Institute for Marine and Atmospheric research Utrecht, Utrecht University, Utrecht, The Netherlands
2 Department of Geoscience & Remote Sensing, Delft University of Technology, Delft, The Netherlands

Correspondence to: Sarah L. Bradley (d80ngv@gmail.com)

Abstract. Observational evidence, including offshore moraines and sediment cores confirm that at the Last Glacial maximum (LGM) the Greenland ice sheet (GrIS) grew to a significantly larger spatial extent than seen at present, grounding into Baffin Bay and to the continental shelf break. Given this larger spatial extent and it is close proximity to the neighboring Laurentide (LIS) and Innuitian Ice sheet (IIS), it is likely these ice sheets will have had a strong non-local influence on the spatial and temporal behaviour of the GrIS. Most previous paleo ice sheet modelling simulations recreated an ice sheet that either did not extend out onto the continental shelf; or utilized a simplified marine ice parametersiation and therefore did not fully include ice shelf dynamics, and or the sensitivity of the GrIS to this non-local signal from the surrounding ice sheets.

In this paper, we investigated the evolution of the GrIS over the two most recent glacial-interglacial cycles (240 kyr BP to present day), using the ice sheet-ice shelf model, IMAU-ICE and investigated the influence of the LIS and IIS via an offline relative sea level (RSL) forcing generated by a GIA model. This RSL forcing controlled via changes in the water depth below the developing ice shelves, the spatial and temporal pattern of sub-ice shelf melting, which was parametrised in relation to changes in water depth.

In the suite of simulations, the GrIS at the glacial maximums coalesced with the IIS to the north, expanded to the continental shelf break to the south west but remained too restricted to the north east. In terms of an ice-volume equivalent sea level contribution, at the Last Interglacial (LIG) and LGM the ice sheet added 1.46m and -2.59m to the budget respectively. The estimated lowering of the sea level by the Greenland contribution is considerably more (1.26 m) than most previous studies indicated whereas the contribution to the LIG high stand is lower (0.7 m). The spatial and temporal behaviour of the northern margin was highly variable in all simulations, controlled by the sub surface melt (SSM), which was dictated by the RSL forcing and the glacial history of the IIS and LIS. In contrast, the southwestern part of the ice sheet was insensitive to these forcing's, with a uniform response in an all simulations controlled by the surface air temperature (SAT) forcing, derived from ice cores.

Clim. Past Discuss., https://doi.org/10.5194/cp-2017-132
Manuscript under review for journal Clim. Past
Discussion started: 16 October 2017

Climate of the Past Discussions
Open Access
EGU

1. Introduction

There have been many previous ice sheet modelling studies of the glacial- interglacial evolution of the Northern hemisphere ice sheets (NHIS) (including the Greenland Ice sheet (GrIS) and/or Laurentide Ice Sheet (LIS) (Helsen et al., 2013;Ritz et al., 1996;Quiquet et al., 2013;Greve et al., 1999;Charbit et al., 2007), in which there was no expanse of the ice sheet beyond the present day (PD) coastline during glacial periods. The ice sheet model in these studies modelled solely the evolution of grounded ice, where the edge of the grounded ice margin was determined based upon by the flotation criterion. However, the wealth of new observational data infers that at glacial maximums the GrIS extended beyond the PD coastline, grounding out onto the continental shelf (Vasskog et al., 2015 and references therein Sect. 2). This shows there is a mismatch between the observed extent and the modelled extent in the above-mentioned models.

A review publication by Dutton et al., 2015 stated that the exact magnitude and contribution of the various global ice sheets to ice-volume equivalent sea level (ESL) during the Last Interglacial (LIG,130-115 kyr BP) is still largely unresolved. From analysis of far-field sea level records, it is estimated to have reached a peak between 6-9 m above PD. However, the precise contribution from the GrIS is poorly constrained and ranges based on ice sheet models between 0.6 and 3.5m (Helsen et al., 2013;Stone et al., 2013;Dutton et al., 2015;Cuffey and Marshall, 2000;Robinson et al., 2011), within in addition a highly variable spatial extent (Vasskog et al., 2015).

Also, Clark and Tarasov, 2014 highlight that closing the Last Glacial Maximum (LGM) ESL budget is now also becoming increasing problematic. This is mostly due to the reduction in the estimated contribution from the Antarctic Ice sheet (AIS), derived from both modelling and/or observational studies. Glacial Isostatic Adjustment (GIA) modelling studies have estimated the contribution of the GrIS to the LGM ESL budget to be ~ 5m (Lecavalier et al., 2015); ice sheet modelling based studies indicate significantly less, typically < 2.5 m (average < 1m) (Fyke et al., 2011;Ritz et al., 1996;Letreguilly et al., 1991). The lower values are possibly caused by restricting the glacial maximum extent to the PD coastline. Consequently, ice sheet modelling based studies which simulate a sufficiently large GrIS during glacial periods, both in terms of maximum spatial extent and total contribution to the ESL sea level budget do not yet exist and resolving the GrIS ESL contribution over the last two glacial remains problematic.

There have been two ice sheet modelling based approaches to address the expansion of the grounded ice sheet beyond the PD margin. In the first approach, often referred to as *a marine parameterisation*, ice is permitted to flow and ground beyond the PD coastline to a specified 'critical water depth', regardless of the ice thickness. This critical water depth is either a function of changes in ESL or constrained by a series of masks reconstructed from observational data sets (Zweck and Huybrechts, 2005). This approach has been adopted in many sheet-only ice sheet modelling studies, solving only for grounded ice and reconstructed an extended GrIS during glacial periods (i.e (Huybrechts, 2002;Simpson et al., 2009;Lecavalier et al., 2014). However, rather than the ice sheet evolving freely, it is preconditioned to match with the observational data and does not use any physically based principles.

Clim. Past Discuss., https://doi.org/10.5194/cp-2017-132
Manuscript under review for journal Clim. Past
Discussion started: 16 October 2017

The second approach includes ice shelves dynamics in combination with a calculation of sub-ice shelf melting (SSM). The sub-ice shelf melt is calculated by a parametersiation which is typically based on changes in water depth, estimated using an ESL forcing. This heuristic approach allows the ice sheet to expand onto the continental shelf but not into the open ocean. There have been a number of publications which applied the second approach using, for instance the GRISLI ice sheet model (Ritz et al., 2001). For example, Colleoni et al., 2014 parameterised the SSM as a uniform value in relation to changes in water depth to examine the growth of the NHIS during MIS7 and MIS5. At glacial periods the reconstructed GrIS grounded across the Nares Strait, the Smith Sound and out onto the continental shelf to the NE and SW (see Fig.8, Colleoni et al., 2014). Although in this reconstruction the ice sheet retreated from the latter two offshore regions (NE and SW) by the LIG minimum (~ 115 kyr BP), it remained grounded across the Nares Strait, which is contrary to the observational data which are reviewed in Sect. 2.

Implicit in both these approaches is that the changes in paleo water depth surrounding the ice sheet are driven by the ESL forcing, generally derived from a benthic $\partial^{18}O$ record (Lisiecki and Raymo, 2005) or by an inverse forward modelling approach (Bintanja and van de Wal, 2008). However, sea level variations are in fact not simply ESL (i.e with no spatial variation), but vary spatially due to numerous processes that dominate over different time scales (Rovere et al., 2016;Kopp et al., 2015), with GIA the dominant processes on the time scales of this study.

This study will advance the second approach, using an ice sheet-ice shelf model 'IMAU-ICE' (Sect. 3.1). The GrIS will be simulated over two glacial cycles (240 kyr BP to PD), focusing on a range of possible parameterisations for SSM (Sect. 3.2). Secondly, to investigate the influence of the spatial and temporal variability in sea level (or water depth) on the GrIS evolution, an offline forcing derived from a GIA model (Sect. 3.3) will be included. The first goal is to investigate if a larger than present day GrIS can be simulated for glacial maximum conditions, which is coherent with the observational data (Sect. 2) and thereby address the current mismatch between the ice sheet model and GIA based GrIS reconstructions. Secondly, we aim to evaluate the spatial and temporal sensitivity of the GrIS to changes in the SSM and the sea level forcing. Finally, we will address issues relating to the GrIS contribution to ESL over the last two glacial cycles.

2. Observational data

There have been numerous recent publications which have reviewed the wealth of (new) observational data that can be used to constrain the spatial and temporal history of the GrIS reconstructed from ice sheet model simulations (e.g Funder et al., 2011; Vasskog et al., 2015; Cofaigh et al., 2016). It is not the aim of this study to replicate this information, rather a selection of studies are outlined below which are particular useful to constrain the ice sheet model simulations (summarised on Table1, Fig.1).

There are currently six Greenland ice core records (Fig.1, white circles) that contain evidence for LIG age ice, which can be used to constrain the minimum extent that the ice sheet reached during LIG (Fig.1). Only simulations where these six sites remained glaciated at the LIG were considered valid. From the NEEM record (Dahl-Jensen et al., 2013) it is inferred that at 122 kyr BP, the surface elevation thinned by 130 ± 300 metres. The other five ice core sites remained ice covered, including

Clim. Past Discuss., https://doi.org/10.5194/cp-2017-132
Manuscript under review for journal Clim. Past
Discussion started: 16 October 2017

Dye-3 (Yau et al., 2016). Additionally, analysis of Sr-Nd-Pb isotope ratios in offshore material collected from Erik Drift (Colville et al., 2011) supports a smaller than present day retreat of the southern margin and indicated that the ice sheet did not undergo complete deglaciation at the LIG.

Constraining the offshore extent at the Penultimate Glacial maximum (PGM) or earlier glaciations is complicated as the older geomorphological evidence (i.e moraines) are overridden by the subsequent readvances. As a consequence, the preservation of offshore sediments is limited. Therefore, we assumed that ice extent during the PGM equals the extent during the LGM. The aim with all simulations within the study was to reproduce a spatially expanded grounded ice sheet which reached the constraints given below during these two glaciations.

Offshore geomorphological evidence collected from numerous geophysical surveys indicate that the ice sheet grounded out onto the continental shelf (Table1, Fig.1), specifically to the shelf break along the SW and north and central east at the LGM. This evidence includes moraines, grounding zone wedges (Hogan et al., 2016), large scale glacial lineation's (Cofaigh et al., 2004) and glacio-marine sediments dated and analysed from offshore cores (Jennings et al., 2006). Table1 provides an overview of the asynchronous nature of the timing of retreat from the glacial maximum towards the PD margin.

Through the expanse of Petermann and Humboldt Glacier at the NW margin out into the Kane and Hall Basin and the Nares Strait (Fig.1), the ice sheet coalesced with the Innuitian Ice sheet (IIS) at the glacial maximums (LGM or PGM). The grounded ice margin reached south into the north of Baffin Bay and out along the Arctic coastline to the north. Dating from one of the few sediment cores from the offshore NW margin (Table1), Jennings et al., 2011 documented that the retreat of the grounded ice from the Kane and Hall Basin initiated after 10.3 kyr BP. The margin retreated in an 'unzipping manner', first from west (Kane Basin) and later to the east (Hall Basin), driven in part by the retreat of IIS back onto Ellesmere Island. The final opening of the connection between the Arctic Ocean and Baffin Bay, via the Nares Strait did not occur until after 9 kyr BP, implying that this region was one of the last regions to deglaciate. The retreat of the grounded ice sheet across the Nares Strait and back to the PD margin was a key feature which was used to constrain the simulations, and if ice remained grounded across this margin at PD, the model simulation was rejected.

Along the NE margin, Evans et al., 2009 concluded that the ice sheet advanced out onto the middle to outer shelf, covering the Westwind trough (open blue square, Fig.1). It grounded close to (as indicated by ice-rafted debris (IRD)) but did not extend as far as the Fram Strait, limited by the continental shelf break (see Fig.1). No dated material was recovered so the timing is unresolved.

Progressing further south, the lateral extent and timing are better constrained (Table1) due to the greater availability of data. Retreat from the central east outer shelf initiated by ~ 15 kyr BP (blue star, Fig.1) stabilising on the inner shelf at 10 kyr BP (green star, Fig.1) and reaching the PD margin by 7.4 kyr BP (red star, Fig.1) (Evans et al., 2002;Cofaigh et al., 2004). Along the SE margin, the retreat from the outer to inner shelf is highly asynchronous, with the retreat from the outer Kangerdlugssuaq trough around 17.8 kyr BP (dark blue triangle, Fig.1) (earlier than from the central east), reaching the inner fjord by 11.8 kyr BP at Kangerdlugssuaq (open blue triangle, Fig.1), and by 10.8 kyr BP at Sermilik (red cross, Fig.1). It is suggested that the timing of retreat across this region is strongly influenced by the warm incursion of Irminger current (Dyke et al., 2014).

Clim. Past Discuss., https://doi.org/10.5194/cp-2017-132
Manuscript under review for journal Clim. Past
Discussion started: 16 October 2017

Climate of the Past Discussions
Open Access
EGU

The SW region of Greenland, around Disko Bugt and Uumannaq trough is one of the more extensively studied region of the ice sheets, with a range of observational data confirming the grounding of the ice sheet to the continental shelf break (Winsor et al., 2015;Sheldon et al., 2016;Jennings et al., 2014;Cofaigh et al., 2013). The retreat from the outer shelf (cluster of red triangles, Fig.1) between 19.3- 18.6 kyr BP is inferred to have been driven by either a change in sea level and/or an ongoing gradual rise in boreal summer insolation rather than changes in ocean temperatures. The margin stabilised at the middle shelf, Hellefiske moraine (open red circle, Fig.1) retreating at 12.24 kyr BP, reaching the inner shelf by 10.9 kyr BP. The question of whether a change in sea level could initiate such a retreat is just one aspect that the use of a RSL forcing in this study will examine. The retreat from the outer shelf edge in the vicinity of the Uumannaq fjord (cluster of green triangles, Fig.1) was later, after 14.9 kyr BP, reaching the outer Uumannaq trough by 10.8 kyr BP (Sheldon et al., 2016).

Against this background of geological evidence, we evaluated our model results as presented in Sect. 4 and later.

3. Method.

3.1. IMAU-ICE: ice sheet-ice shelf model.

As the aim of this study is to simulate the expansion and retreat of the GrIS onto the continental shelf, it is essential to utilise an ice sheet model which includes the possibility for ice shelves to ground and thereby the ice sheet expanding beyond the PD margin. To achieve this, we used a 3D thermomechanical ice sheet-ice shelf model IMAU-ICE (previously known as ANICE) (Helsen et al., 2013;Helsen et al., 2012;Graversen et al., 2011;de Boer et al., 2014;Bintanja and van de Wal, 2008;van de Wal, 1999b, a). For regions of grounded ice, IMAU-ICE uses the commonly adopted SIA approximation (Hutter, 1983) to simulate ice velocities in combination with a 3D thermodynamical approach. The ice shelf velocities are approximated using the SSA solution (Macayeal, 1989). The model distinguishes ice sheet (grounded) and ice sheet points using the flotation criterion. The complex marginal topography of Greenland, with narrow troughs with steep gradients, can lead to complications when adopting the usual SSA approach. To address this problem, a 2D one-sided surface height gradient discretisation scheme was included for ice shelf points neighbouring the grounded line.

Present day topographic input fields of ice thickness, surface elevation and bed topography are taken from Bamber et al., 2013 with input climate fields (surface mass balance (SMB), refreezing, surface air temperature (SAT)) adapted from the RACMO2 dataset (van Angelen et al., 2014). All these external datasets are interpolated and projected onto the 20x20km ice model grid using the mapping software OBLIMAP2.0 (Reerink et al., 2010;Reerink et al., 2016). The adopted OBLIMAP grid projection parameters were λ =371.5, ϕ=71.8 and α=7.15. Adjustment of the SMB due to elevation changes driven by the evolution of the ice sheet are accounted for by the 'SMB gradient method' (Helsen et al., 2012).

Two suites of simulations were conducted: (i) sheet-only, where IMAU-ICE was ran without the inclusion of shelves. This is similar to as was adopted in previous GrIS studies using ANICE (Helsen et al., 2013) and will be taken as a reference, (ii) with shelves where IMAU-ICE was ran with

Clim. Past Discuss., https://doi.org/10.5194/cp-2017-132
Manuscript under review for journal Clim. Past
Discussion started: 16 October 2017

Climate of the Past Discussions

the inclusion of ice shelves. For both these suites of simulations, the following modelling procedure was adopted. First, IMAU-ICE was ran for 100 kyr, under a constant present day climate, to reach an equilibrium state with the aim of replicating the observed present day configuration (Bamber et al., 2013). The sensitivity to the flow enhancement factor (m_{enh}, varied between 1-5) was investigated for a range of sliding coefficients (A_s) values (0.04 to 1.8×10^{-10} m^8N^{-3} yr^{-1}). The resultant ice volume varied over the range of m_{enh} and A_s by ~ 0.12×10^{15} m^3, with all simulations producing an underprediction across the centre of the ice sheet and overprediction at the narrow outlet glaciers, a feature common to SIA models. Based on this preliminary evaluation a value of m_{enh}=3.5 was used in all simulations. Secondly, each simulation was ran for 240 kyr using a SAT forcing (Helsen et al., 2013) (Fig. S1) combined with a SSM parametrisation and sea level forcing, to simulate the GrIS evolution over the two glacial cycles. Four SSM parameterisations were investigated (see Sect. 3.2, Fig.2 and Fig.S2), where for each parameterisation a range of parameters were investigated. Two possible sea level forcing's were investigated (Sect. 3.3), either an ESL forcing (Fig.S1) which was taken from Bintanja and van de Wal, 2008 or a RSL forcing (Sect. 3.3) derived from GIA modelling This resulted in a final suite of ~ 300 simulations which were evaluated using the observational data defined in Sect. 2.

3.2. Parameterisation of sub-ice shelf melt (SSM)

As full physical based models including sub ice shelf are still under development four sub-ice shelf melt (SSM) parameterisations of increasing complexity were investigated for the simulations with shelves (Fig.S2, Fig.2). They are all primarily based around the assumption (Sect. 1) that for an increase in paleo water depth (or sea level) there will be a corresponding increase in the amount of SSM. Hence the SSM does not depend on temperature: temperature changes only affect surface mass balance changes.

Method 1: 'Constant SSM' assumes a uniform SSM (given by SSM1) at all water depths, following the approach used in Nowicki et al., 2013. Method 2: 'Stepped SSM' follows the approach used by Colleoni et al., 2014 (see Sect. 1), with a sharp stepwise increase in SSM at a certain water depth (WD), from SSM1 to SSM2. Method 3: 'Exponential and constant' reproduces an exponential increase in SSM with water depth. The SSM increases up to a certain water depth, WD1, at which point there is a sharp increase in the SSM to a constant value, SSM2.

Method. 4: 'Exponential' will be the main parameterisation investigated (Fig.2). In this method, the SSM increases with water depth (WD) by a power law relation with a constant a, and exponent m.

$$SSM = a.WD^m \quad (1)$$

In order to conveniently fit this power law through two points (SSM1, WD1) and (SSM2, WD2), we solve:

$$m = \frac{ln\left(\frac{ssm2}{ssm1}\right)}{ln\left(\frac{WD2}{WD1}\right)}; \quad a = \frac{ssm1}{WD2^m}; \quad (2)$$

The range of parameter values for SSM1, SSM2 and WD1 (water depth1) and WD2 (water depth2) adopted are listed in Table2 for each Method (Fig.2).

Clim. Past Discuss., https://doi.org/10.5194/cp-2017-132
Manuscript under review for journal Clim. Past
Discussion started: 16 October 2017

Climate of the Past Discussions
Open Access
EGU

3.3. Sea Level or Water Depth forcing

Sea Level (or water depth), WD(θ,ψ,t) can be defined as the vertical distance between the equilibrium ocean surface, the geoid $G(\theta,\psi,t)$ and the solid earth surface $R(\theta,\psi,t)$ (bed topography) (Mitrovica and Milne, 2003). A change in the water depth $\Delta WD(\theta,\psi,t)$ can result from any vertical deformation in these two surfaces, and is defined as:

$$\Delta WD(\theta,\psi,t) = \Delta G_T(\theta,\psi,t) - \Delta R_T(\theta,\psi,t) \quad (3)$$

Where $G_T(\theta,\psi,t)$ and $R_T(\theta,\psi,t)$ are the vertical perturbations in the geoid and solid earth surface, at θ co-latitude, ψ east-longitude and time t.

In this study two different sea level (or water depth) forcing's are incorporated into IMAU-ICE to examine the influence of spatial and temporal variability in ΔWD via the SSM parameterisation on the expansion and retreat of the GrIS.

The first method is commonly used in ice sheet modelling studies. It applies a spatially uniform, time varying ESL forcing to represent the perturbations in the geoid/ocean surface. The adopted forcing in this study was taken from Bintanja and van de Wal, (2008) (Fig.S1). The deformation of the solid earth ($R(\theta,\psi,t)$) was calculated using the elastic lithosphere-relaxing asthenosphere (ELRA) method (Le Meur and Huybrechts, 1996) internally within IMAU-ICE. Typically, in the near field regions (across previously glaciated locations), it is the deformation of the solid earth surface resulting from the local changes in ice in Greenland, and ocean loading history that primarily drive the changes in sea level (water depth). This method which will be referred to as ESL forcing.

However, in reality the water depth/sea level signal surrounding the GrIS is highly spatially variable, and more complicated than as represent by an ESL forcing. On the time scales of this study the main processes driving this spatial variability is GIA (Rovere et al., 2016). The spatial variability in the signal is in part driven by local changes in the GrIS, as is typical for near field regions and to non-local changes driven by the LIS (Lecavalier et al., 2014). This is because Greenland sits on the resulting forebulge of the LIS. Ideally, the most complete method of incorporating this complex spatial pattern on the evolution of the GrIS would be with a coupled ice sheet- GIA model, as in de Boer et al. (2014). Instead, a simpler alternative method was adopted in this study, by incorporating an offline coupling with the output of a GIA model. This second method will be referred to as RSL forcing.

To incorporate the output from the GIA model, first Eq. (3) was decomposed into (a) a local (subscript L) signal, driven by changes in the GrIS ($\Delta G_L, \Delta R_L$) and (b) a non-local signal driven by the influence of all other ice sheets, primarily the LIS ($\Delta G_{NL}, \Delta R_{NL}$). Hence the change in water depth is:

$$\Delta WD(\theta,\psi,t) = \left(\Delta G_L(\theta,\psi,t) + \Delta G_{NL}(\theta,\psi,t)\right) - \left(\Delta R_L(\theta,\psi,t) + \Delta R_{NL}(\theta,\psi,t)\right) \quad (4)$$

In order to solve this relationship for water depth a GIA model was used to calculate the non-local contributions (ΔG_{NL} (Fig.3d) and ΔR_{NL} (Fig.3a)). This model has three user defined input components: a reconstruction of Late Pleistocene ice sheet history (Peltier, 2004), an Earth model that simulates the solid earth deformation due to changes in the surface mass redistribution between the oceans and ice sheets (Peltier, 1974) and a model of sea-level change (Farrell and Clark, 1976). The sea-level model adopted included perturbations to the rotation vector (Mitrovica et al., 2001;Mitrovica et al., 2005;Milne and Mitrovica, 1998), time-dependent shoreline migration and an accurate treatment of

Clim. Past Discuss., https://doi.org/10.5194/cp-2017-132
Manuscript under review for journal Clim. Past
Discussion started: 16 October 2017

Climate of the Past Discussions
Open Access
EGU

sea-level change in areas characterised by ablating marine based ice (Kendall et al., 2005;Mitrovica and Milne, 2003).

To run the GIA model over the two glacial cycles (240 kyr to PD), an input global ice reconstruction is required which reproduces the spatial and temporal history of all global ice sheets, apart from the GrIS during this interval. As a basis for this reconstruction, the ICE5G global ice model (Peltier, 2004) was adopted, which extends from 122 kyr BP to PD; one glacial cycle. As the history for two glacial cycles was required, the ice history over the 122 kyr was duplicated to represent the previous glacial-interglacial cycles (240 kyr to 122 kyr BP), resulting in an ice sheet reconstruction from 240 kyr to PD. The GrIS component was removed from ICE5G to produce the final 'non-local' input ice history.

The adopted earth model is characterised by a 96 km lithosphere, and upper and lower mantle viscosity values of 5 $\times 10^{20}$ Pa s and 1×10^{22} Pa s, respectively. These viscosity parameters fall approximately within the middle of the range of values commonly inferred. Using this input ice history and earth model the GIA model was ran offline to produce the non-local geoid and deformation fields (ΔG_{NL} (Fig.3d) and $+\Delta R_{NL}$ (Fig.3a).

As the GIA model is used to produce the non-local components, the 'local' fields (ΔR_L , ΔG_L) are still required to solve Eq. (4). The local driven changes in the solid earth surface, ΔR_L were calculated internally within IMAU-ICE, using the ELRA method (Le Meur and Huybrechts, 1996) (Fig.3b). This is the same approach as used with the ESL forcing. This local field is combined with ΔR_{NL} (from the GIA model) to calculate the total deformation of the solid earth ΔR_T (Fig.3c) at each time step.

Referring back to Eq. (4), using this method result in the following revised equation for ΔWD:

$$\Delta WD(\theta, \psi, t) = \left(\Delta G_{NL}(\theta, \psi, t)\right) - \left(\Delta R_L(\theta, \psi, t) + \Delta R_{NL}(\theta, \psi, t)\right) \quad (5)$$

Comparing Eq. (4) to Eq. (5), it is evident that the local geoid, G_L is not included here. The magnitude of this missing signal can be calculated by taking the difference between the total signal (Fig.3f, derived from Eq.4) and the signal as obtained from Eq.5 (Fig.3e). This difference, 'the local geoid' is small (contoured on Fig.3f), but is a shortcoming of the modelling that is accepted given the simplicity of other component of the model. It is noted that this approach neglects for example feedbacks between changes in the sea level and the marine-based ice and the stabilizing influence this may have on the evolution of the ice shelves (Gomez et al., 2010;de Boer et al., 2014).

As the Fig.3a illustrates, at the PGM there is a significant non-local deflection in the solid earth surface. Across Ellesmere Island and the NW Greenland, the LIS and IIS produces significant subsidence, up to 200 m with central Greenland and Baffin Bay elevated by up to 100 m and 30 m respectively, due to the influence of the forebulge. In contrast, the non-local geoid signal is much smaller, with a range of ~ 40 m (Fig.3d). Comparing these two signals, it is apparent that it is the deflection of the solid earth surface, which will be the main contributor to driving changes in RSL (Fig.3e and 3f).

Clim. Past Discuss., https://doi.org/10.5194/cp-2017-132
Manuscript under review for journal Clim. Past
Discussion started: 16 October 2017

Climate of the Past Discussions
Open Access
EGU

4. Results for simulations using sheet-only IMAU-ICE.

In this Sect., results of the sheet-only simulations are discussed. Using the RSL forcing (compared to the ESL forcing) resulted in only a minor difference to the total ice volume (TableS1a, b), but significant spatial differences (Fig.4e, f g and h). The total LIG and LGM ESL contribution, including the RSL forcing is ~ 1 m and -1m respectively (1.24 and -1.17m with ESL forcing (TableS1c)) which is at the lower end of the current range of estimated for the GrIS (see Sect.1). None of the simulations produced an ice sheet that expanded beyond the PD coastline to reach the offshore limits as defined by the observational data (Fig.4a, c). This implies that some additional method that enables the ice sheet to extend beyond the PD coastline is required.

During glacial periods (Fig.4a and c), including the RSL forcing results in a significant thinning across the NW, near the Humboldt and Petermann glaciers (> 400m) which was caused by local uplift driven by the growth of the LIS (Fig.3a), and in turn reduction in the bedrock height. This local thinning is compensated by a central thickening, ~ 50 m, which combined results in only a minor reduction in the total ice volume at the glacial maximum, ~ 0.08 $\times 10^{15}$ m^3 (relative to ESL forcing). At the LIG minimum, the retreated SW margin in thicker (Fig.4f) due to a reduction in the relative uplift and hence a deeper bedrock (relative to ESL forcing). The local uplift which is generated by the GrIS inland retreat, thinning and unloading is overprinted by the 'non-local' driven subsidence, whereas the LIS retreats and the associated forebulge subsides, the local bedrock deepens. It is this combination of local and non-local signals that reduces the bedrock depth relative to adopting only the ESL forcing. As a consequence, an inland retreat of the SW margin is produced in all simulations, but the lateral inland extent is highly sensitive to the choice of sliding coefficient, A_s which is linearly related to the velocity of the ice; with a progressive increased retreat as the A_s parameter is increased from 0.04 $\times 10^{-10}$ to 1.8×10^{-10} $m^8N^{-3}yr^{-1}$ (which is equivalent to a reduction in the bed roughness). Up to an $A_s \leq 1.2\times10^{-10}$ $m^8N^{-3}yr^{-1}$, the SW margin retreats to a smaller than PD extent but all LIG ice cores sites remained ice covered (Fig.4c). With an $A_s > 1.2\times10^{-10}$ $m^8N^{-3}yr^{-1}$ the retreat was too extreme, with the DYE3 ice core deglaciated. Based on these results, a maximum A_s of 1.2×10^{-10} $m^8N^{-3}yr^{-1}$ was adopted in all simulations with ice shelves.

The simulated PD ice sheet is relatively insensitive to the choice of sea level forcing (Fig.4h) or A_s value, with consistent misfits in all simulations. Increasing the basal sliding (a lower A_s) resulted in an increase in the inland retreat along the SW, NE and NW margin and underprediction of the observed surface elevation (Fig.4g). Conversely, there is a reduction in the central and northern overthickening. Therefore, there is a trade-off in the choice of A_s to optimise between these two results: reducing the central overthickening and reducing the SW inland retreat. The pronounced overthickening along most of the coastline in the reconstructed PD extent (up to 500m, Fig.S4) is in part due to coarse resolution (20x20km) of the simulations in these narrow outlet fjords. Preliminary investigations increasing the resolution to 10x10km reduced this misfit but a more detailed modelling of outlet glacier at scales down to kilometres is likely to be needed to fully resolve this misfit.

Clim. Past Discuss., https://doi.org/10.5194/cp-2017-132
Manuscript under review for journal Clim. Past
Discussion started: 16 October 2017

Climate of the Past Discussions
Open Access
EGU

5. Results for simulations using with shelves and RSL forcing

5.1. Results for Preliminary SSM parameterisation: Method 1-3.

345 This preliminary suite of simulations investigated the three SSM parameterisation (Method 1-3, Fig.S2, Table2) as adopted in previous ice sheet model based studies of the GrIS. None of the simulations created a glacial-interglacial ice sheet evolution, which over the two glacial cycles was consistent with the observational data (Sect.2, Table 3, Fig.1) i.e an expanse beyond the PD margin, coalescing with the IIS to the NW and an accompanying retreat by the present day. A complete description of these 350 results is provided in Sect. S1, with a few key points that were relevant to the development of Method 4 outlined below.

Regardless of the SSM variation (constant (Method 1, 2), or exponential (Method 3)) up to WD1, a relatively low SSM1 (< 0.75 m/yr) was required to permit the floating ice sheet to thicken, ground and the ice sheet expand beyond the PD margin. Introducing the exponential increase in SSM 355 with water depth (Method 3) resulted in a spatial extent of the ice sheet at glacial maximums more consistent with the observational data. The reconstructed ice sheet was also highly sensitive to the resultant SSM at water depths greater than WD1 (between 400-700m, constrained by SSM2); surrounding the expanded grounded margin. Reducing the SSM close to this expanded margin increased the offshore glacial maximum extent. However, with the use of a constant SSM at these 360 deeper water depth (as in all Methods 1-3), it was still not possible to generate the required interglacial retreat.

As was found with the sheet-only simulations, the spatial and temporal extent was highly dependent on the basal sliding, defined by the choice sliding coefficient, A_s. Adopting a higher A_s increased the spatial extent and thickness at the glacial maximums to produce a GrIS closer to the 365 observed data (Fig.1). The PD reconstruction along the SW margin was improved (relative to sheet-only simulation) as the inland retreat was impeded, resulting in a thicker ice sheet. However, across the NW margin a considerable volume of grounded ice remained.

5.2. Results for optimum SSM parametersiation: Method 4

5.2.1. Influence of RSL forcing on with shelves simulations.

370 Regardless of the choice of parameters adopted in Method 4, there was no simulation where using an ESL forcing produced a glacial-interglacial retreat of the ice sheet. In all simulations, a considerable volume of grounded ice remained across the NW margin (see Fig.5d,5h). Therefore, the inclusion of the RSL forcing was required to drive the ungrounding and retreat of GrIS during interglacial periods. The timing of the expanse and grounding of the ice sheet out onto the continental shelf at the onset of 375 glaciation was slowed with the inclusion of the RSL forcing, reaching a maximum extent across the NW, ~ 20 kyr later. The resultant ice sheet is thinner (Fig.5b and 5f) within the deeper fjords around the southern margin of the ice sheet (i.e. Uumannaq, Kangerdlugssuaq Sermilik Fjord) and to the NW, but thicker across the centre of the ice sheet. However, the maximum spatial extent at the glacial maximum was relatively insensitive to the choice of sea level forcing (RSL or ESL). This spatial 380 variation combines to reduce the total LGM ESL contribution by ~ 0.28 m (relative to ESL forcing).

Clim. Past Discuss., https://doi.org/10.5194/cp-2017-132
Manuscript under review for journal Clim. Past
Discussion started: 16 October 2017

At the LIG minimum (Fig.5d), the inclusion of the RSL forcing (on average) increased the LIG ESL contribution, due to the retreat of the grounded ice sheet across the Nares Strait. However, the inland retreat at the SW margin was impeded, with a thickening along this margin.

The resultant PD extent was highly sensitive to the inclusion of the RSL forcing, specifically via the impact on the spatial and temporal behaviour of the NW margin, in contrast to what was found in the sheet-only simulations (Sect. 4) (see Fig. 4h and Fig. S4). The lateral inland retreat of the SW margin remained relatively unaltered, but the underprediction with respect to the observations along this margin is reduced.

It is the strong influence of the LIS, via the non-local bedrock deformation (Fig.3a) which drives this dominant influence of the RSL forcing, partially in the influence on the spatial and temporal behaviour of the NW margin. The Nares Strait lies close to the hinge-line of the influence of the LIS (Fig.3a, dark blue region): as the LIS ice sheet expands during glacial maximum periods, the bed topography is depressed (relative to the ESL forcing) which in turn will increase the water depth across this offshore region. This will lead to a higher SSM in these region (see Eq.1), slowing the expanse of the GrIS during glacial periods. It is this non-local driven subsidence of the bed topography and in turn higher SSM which causes the more restricted extent across the NW margin with the RSL forcing. During the deglaciation, the retreat and thinning of the GrIS will generate local driven uplift across the same region, which on its own would drive a reduction in the SSM. However, this uplift signal is counteracted by a non-local driven subsidence, as the LIS retreats and its forebulge (which is evident across the main body of the GrIS, Fig.3a) subsides. As these two processes combine during interglacial periods the net effect is to produce a deeper bed topography relative to the ESL forcing only simulations. This results in a higher SSM and promote the retreat of the NW margin in the 11 simulations on Table3.

5.2.2. Final optimum simulations using Method 4.

There were only nine combinations of SSM1, SSM2, WD1 and A_s (Method 4, RSL forcing) from the ensemble of simulations that resulted in glacial – interglacial retreat over the two glacial cycles (Table3) and fulfilled the conditions defined in Sect.2. Two additional simulations are included (LowA_s_lowSSM1-0.25_deep and HighA_s_highSS1) which only resulted in a glacial-interglacial expanse between the LGM and PD. A more detailed description of the sensitivity to each parameter is provided in the Sect. S2.

The average LIG ESL contribution from this selection of 11 accepted simulations is 1.46 m, which lies within the most recent range for the LIG GrIS of between 0.6-3.5 m (Dutton et al., 2015). It is a decrease (on average) of 0.7 m relative to the sheet-only and ESL forcing simulations. All simulations complied with the spatial limits inferred from the LIG ice core data; of a thinning at NEEM (~ 250m) and a moderate inland retreat of the SW margin, but with DYE3 remaining covered with grounded ice. The average LGM ESL contribution is -2.59 m, an increase of 1.26 m relative to the sheet-only and ESL forcing simulations. This is at the upper limit relative to previous ice sheet modelling based studies (Fyke et al., 2011), but remains still ~50% smaller than estimates from GIA

Clim. Past Discuss., https://doi.org/10.5194/cp-2017-132
Manuscript under review for journal Clim. Past
Discussion started: 16 October 2017

modelling based studies (i.e Lecavalier et al., 2004). The use of the with shelves and RSL forcing improved the fit to the glacial maximum observed data (Fig.1, relative to sheet-only and ESL forcing), reaching the inferred limits along the northern and eastern margin. However, at SW margin (see red and green triangles, Fig.5a and 5c) the ice sheet remains too restricted, possibly related to a too strong mass balance height feedback in this region.

There is an evident correlation between the temporal variability of SAT forcing and the total ice volume in all simulations (Fig. S5 and Fig.6); the periods of maximum ice volume (PGM, LGM) corresponding with the minimum in SAT and vice versa (Fig.S1). This would imply that the timings of the glacial-interglacial variations are strongly dependent on the adopted SAT forcing. However, there is a spatially variable response between the NW and SW margins which alludes that the two regions are responding regionally to a different forcing mechanism or at least a different timing of the same mechanism. The interplay between the SAT and RSL forcing and the spatial and temporal variability in ice sheet margin will be examined in greater detail for the last 20 kyr BP (see Sect. S3 for the interplay over the complete 240 kyr interval).

There is very little variation in total ice volume and spatial extent between the nine simulations from the LGM (~ 19 kyr BP) to 14.6 kyr BP (Fig.6, Fig. S5). This corresponds to a period of relatively stable SAT ~ -15°C and minimal variations in the non-local RSL forcing (either the predicted bedrock depth or sea surface height (Fig.3)) with only minor changes in the LIS (Peltier, 2004). Following this, there are three time periods (shaded region on Fig.6) where changes in the ice volume and SAT correlate with a significant retreat/readvance along the SW, SE and to a lesser extent NE (Fig.7), but a static NW margin. Between 14.6 kyr BP (Fig.7) and ~13.9 kyr BP there is a rapid retreat in the grounded SW margin (Fig.6, Fig.7a-b) and a fall in ice volume of ~ 1.0×10^{15} m^3(~ 0.24m ESL). This coincides with a sharp rise in SAT of ~ 10°C (Fig.6) and a strong non-local RSL signal due to a significant retreat of the LIS. As the LIS deglaciated, this will induce non-local subsidence of the bedrock (Fig.3) across this margin, increasing the water depth and in turn the SSM. During this period of retreat, there is little variation in the grounded ice extent to the north and south east. Following this retreat, there is a ~ 1 kyr stillstand in the grounded ice extent (Fig.7c), during which there is a slow gradual cooling in the SAT (Fig.7c). From ~12.9 till 11.5 kyr BP (Fig.6, Fig.7d) correlating with a fall in SAT of ~ 15°C the ice sheet readvances along the SW to produce a small increase in total ice volume (largest in simulations with high A_s). With the onset of the sharp rise in SAT of ~12°C at 11.5 kyr BP, the main period of retreat towards the PD margin begins (Fig.7d-g). This readvance occurs in combination with a large non-local RSL signal, as the LIS undergoes it's final period of deglaciation. This implies that changes in the SSM (driven by the RSL signal) have only a secondary influence of the dynamics of the SW margin. This is emphasised by the minimal variations in the behaviour of the SW margins between the nine final simulations. In Sect. 2, from analysis of observational data, it was inferred that the retreat from this margin may, in part be driven by the changes in RSL forcing. The simulation carried out in this study suggest that this is not the case, with the retreat driven primarily responding to the SAT forcing.

The spatial and temporal behaviour of the NW margin (blue box, Fig.1) in all 11 simulations (Table 3) is highly variable, correlating with changes in the SSM, driven by the non-local and local

Clim. Past Discuss., https://doi.org/10.5194/cp-2017-132
Manuscript under review for journal Clim. Past
Discussion started: 16 October 2017

Climate of the Past Discussions
Open Access
EGU

RSL forcing. There is minimal relation to the timings of the SAT forcing. In all simulations, the timing of final deglaciation of this NW margin was too late (~ 10- 9 kyr BP from observations), but the spatial pattern as inferred by Jennings et al. (2011), of an inwards retreat initiated at the western margin first and later to the east is replicated. This (as described in Sect. S2) is due to the faster ice velocity within the narrow outlet fjords to the west, ie Humboldt glacier, which feed into the grounded ice sheet across the Kane Basin (relative to the eastern grounded margin cross the Hall Basin). The initiation of this retreat was controlled in part by the timing of the final deglaciation of the LIS within the ICE5G model (Peltier, 2004); with retreat across Hudson Bay at 10 kyr BP, and complete deglaciation of the high Arctic by ~ 8 kyr BP. This drives the onset of the non-local subsidence of the bedrock across this region (Fig.3a and 3c), as the LIS forebulge collapses (Sect. S2). It is noted that changes in the choice of earth model and/or the spatial and temporal deglaciation history of the LIS during this final deglaciation interval will of course directly impact on the timing of the GrIS retreat.

The amount of basal sliding (via the choice of A_s) also influences the timing of the onset of this retreat: with a lower amount of basal sliding (simulations with an average A_s, Av A_s Table3,) generally promoting an earlier retreat (relative to the high A_s). For example, retreat is initiated 5 kyr earlier in the simulation A_vA_s_lowSSM1-0.5_shallow than HighA_s_lowSSM1-0.25 (Fig.8, see Table3). In part the delay in the onset of retreat with a higher A_s is due to more expansive and thicker grounded ice sheet, so there is larger volume of ice to retreat (compare Fig.8a and Fig.8d) but also the different Method 4 SSM parameters. In A_vA_s_lowSSM1-0.5_shallow the combination of a higher SSM1 (0.5 m/yr c.f 0.25 m/yr) and a shallower WD1 (300m c.f 475m) shifts the transition in the critical water depth. The resultant SSM is > 0.5 m/yr up to 300 m and > 10 m/yr at depths > 600 m, at the edge of the expanded ice margin. This higher SSM at all water depths, combined with the lower A_s drives the earlier onset of retreat and more restricted glacial maximum extent (Fig.8a).

The choice of Method 4 SSM parameters (see Table.3) combined with the influence of the non-local RSL forcing, also strongly governed the timing of this NW retreat in other simulations (Sect. S2). For example, given the lower SSM1 (0.25 m/yr c.f 0.5 m/yr) in the simulation HighA_s_lowSSM1-0.25 compared to HighA_s_lowSSM1 (see Table 3), it would be assumed that as the resultant SSM will be lower at a given water depth close to the edge of the ice margin and this would delay the onset of retreat. However, the retreat is in fact 1 kyr earlier. This is due to the non-local influence of the IIS (which develops across the Ellesmere Island) on the behaviour of this region. In this simulation (HighA_s_lowSSM1-0.25) the IIS is considerably thicker (> 1500m), increasing the depression of the bedrock (due to the increased ice loading), the water depth and in turn producing a higher SSM which drives the earlier deglaciation. This highlights the influence of the IIS on controlling the deglaciation of the GrIS across this region.

The SSM at deeper water depths, controlled by SSM2 also strongly influences the behaviour of the NW margin. With a lower SSM2 (Eq.2 and described in Sect. S2), the SSM at a given water depth is reduced, again implying that the onset of retreat would be delayed. However, when SSM2 was reduced by 25 m/yr between simulations AvA_s+A_vSSM1 and AvA_s+A_vSSM1_redSSM2, the onset of retreat was 1 kyr earlier; the latter simulation has the earliest onset of retreat from all results (see Table3). This is a result of the influence of the PGM to LIG history (first glacial-interglacial cycle) on

Clim. Past Discuss., https://doi.org/10.5194/cp-2017-132
Manuscript under review for journal Clim. Past
Discussion started: 16 October 2017

the dynamics of the LGM to PD retreat. During the first advance of the ice sheet along this margin (up to the PGM), due to the lower SSM at water depths > 400 m, a thicker ice sheet develops across the Nares Strait and eastern Ellesmere Island. This increases the non-local bedrock subsidence, the water depth and produces a higher SSM in the subsequent readvances following the LIG minimum (see Fig.S6a). This higher SSM slows the onset of this readvance (by 30 kyr) and restricts the spatial extent of the grounded ice margin to the central Nares Strait (Fig.S6b). As Fig.S6b illustrates, at the onset of retreat, the higher SSM surrounding the grounded ice margin (Fig.S6c) induces the earlier onset of retreat.

6. Conclusions

In this study using the ice sheet-ice shelf model IMAU-ICE, the evolution of the GrIS over the two most recent glacial- interglacial cycles (240 kyr BP to PD) was investigated. The sensitivity of the spatial and temporal behaviour of the ice sheet to an offline RSL forcing, generated by a GIA model was incorporated. Through this, the influence of the glacial history of the LIS and IIS was explored. This RSL forcing governed via changes in the water depth below the GrIS developing ice shelves, the spatial and temporal pattern of SSM. The SSM was parameterisation in relation to the water depth, where for an increase in water depth, the SSM increased.

At the LIG minimum, all of the LIG ice cores remain ice covered, with a ~ 250 m thinning at NEEM and an inland retreat of the SW margin. This contributed 1.46 m to the LIG highstand, a reduction of 0.7 m relative to sheet only simulations combined with a ESL forcing. At the glacial maximums, the ice sheet has expanded offshore to coalesces with the IIS reaching the Smith Sound at the north of Baffin Bay and out onto the continental shelf along the SW but is still too restricted to the NE. A LGM ESL contribution of -2.59m is still low and closing the LGM ESL budget remains problematic. However, this is an increase of 1.26 m relative to the sheet only simulations combined with a ESL forcing.

The temporal response of the SW margin was primarily controlled by the adopted SAT forcing (taken from ice core records). The RSL forcing and the choice of SSM parameterisation were of secondary influence. However, the inclusion of the RSL forcing improved the reconstructed present day GrIS by reducing a underprediction along the SW margin (relative to observations). Conversely the NW margin, where the ice sheet coalesced with the IIS was relatively insensitive to the imposed SAT forcing; instead the spatial and temporal response were controlled by variation in resulted SSM patterns driven by the spatial and temporal variability in the RSL forcing and the glacial history of the LIS and IIS. RSL and temperature change combined to generate a highly variable temporal response, where optimum parameters were found to be a sliding coefficient A_s in the range of 1.0×10^{-10} to 1.2×10^{-10} $m^{8}N^{-3}yr^{-1}$; a relatively low SSM close to the grounded ice margin for an expanse to occur, and a higher SSM at deeper water depths to promote retreat.

Code availability

The IMAU-ICE model is part of the ICEDYN package. The code used in this study is based on the ICEDYN SVN revision 2515. OBLIMAP is an open source package which is available at https://github.com/oblimap/oblimap-2.0

Data availability

Output from all simulations, including the GIA model used for forcing and the RSL forcing used within this study are available from the S.L.B upon request.

Author contribution

The IMAU-ICE model was developed by T.J.R and R.S.W.W. S.L.B performed model simulations and led manuscript writing and study development. All authors contributed to discussion in the study development and writing of the manuscript.

Competing interests

The authors declare that they have no conflict of interest

Acknowledgements

S.L.B and T.J.R acknowledge support from the Netherlands Earth System Science Centre (NESSC), which is financially supported by the Ministry of Education, Culture and Science (OCW). M.M.H was supported by The Netherlands Polar Programme (NPP) of the Earth and Life Sciences division of The Netherlands Organisation for Scientific Research (NWO/ALW).

References

Bamber, J. L., Griggs, J. A., Hurkmans, R., Dowdeswell, J. A., Gogineni, S. P., Howat, I., Mouginot, J., Paden, J., Palmer, S., Rignot, E., and Steinhage, D.: A new bed elevation dataset for Greenland, Cryosphere, 7, 499-510, 10.5194/tc-7-499-2013, 2013.

Bintanja, R., and van de Wal, R. S. W.: North American ice-sheet dynamics and the onset of 100,000-year glacial cycles, Nature, 454, 869-872, 10.1038/nature07158, 2008.

Charbit, S., Ritz, C., Philippon, G., Peyaud, V., and Kageyama, M.: Numerical reconstructions of the Northern Hemisphere ice sheets through the last glacial-interglacial cycle, Climate of the Past, 3, 15-37, 2007.

Clark, P. U., and Tarasov, L.: Closing the sea level budget at the Last Glacial Maximum, Proceedings of the National Academy of Sciences of the United States of America, 111, 15861-15862, 10.1073/pnas.1418970111, 2014.

Cofaigh, C. O., Dowdeswell, J. A., Jennings, A. E., Hogan, K. A., Kilfeather, A., Hiemstra, J. F., Noormets, R., Evans, J., McCarthy, D. J., Andrews, J. T., Lloyd, J. M., and Moros, M.: An extensive and dynamic ice sheet on the West Greenland shelf during the last glacial cycle, Geology, 41, 219-222, 10.1130/g33759.1, 2013.

Cofaigh, C. O., Briner, J. P., Kirchner, N., Lucchi, R. G., Meyer, H., and Kaufman, D. S.: PAST Gateways (Palaeo-Arctic Spatial and Temporal Gateways): Introduction and overview, Quaternary Science Reviews, 147, 1 - 4, http://dx.doi.org/10.1016/j.quascirev.2016.07.006, 2016.

Cofaigh, C. Ó., Dowdeswell, J. A., Evans, J., Kenyon, N. H., Taylor, J., Mienert, J., and Wilken, M.: Timing and significance of glacially influenced mass-wasting in the submarine channels of the Greenland Basin, Marine Geology, 207, 39-54, http://dx.doi.org/10.1016/j.margeo.2004.02.009, 2004.

Colville, E. J., Carlson, A. E., Beard, B. L., Hatfield, R. G., Stoner, J. S., Reyes, A. V., and Ullman, D. J.: Sr-Nd-Pb Isotope Evidence for Ice-Sheet Presence on Southern Greenland During the Last Interglacial, Science, 333, 620, 2011.

Cuffey, K. M., and Marshall, S. J.: Substantial contribution to sea-level rise during the last interglacial from the Greenland ice sheet, Nature, 404, 591-594, 10.1038/35007053, 2000.

Dahl-Jensen, D., Albert, M. R., Aldahan, A., Azuma, N., Balslev-Clausen, D., Baumgartner, M., Berggren, A. M., Bigler, M., Binder, T., Blunier, T., Bourgeois, J. C., Brook, E. J., Buchardt, S. L., Buizert, C., Capron, E., Chappellaz, J., Chung, J., Clausen, H. B., Cvijanovic, I., Davies, S. M., Ditlevsen, P., Eicher, O., Fischer, H., Fisher, D. A., Fleet, L. G., Gfeller, G., Gkinis, V., Gogineni, S., Goto-Azuma, K., Grinsted, A., Gudlaugsdottir, H., Guillevic, M., Hansen, S. B., Hansson, M., Hirabayashi, M., Hong, S., Hur, S. D., Huybrechts, P., Hvidberg, C. S., Iizuka, Y., Jenk, T., Johnsen, S. J., Jones, T. R., Jouzel, J., Karlsson, N. B., Kawamura, K., Keegan, K., Kettner, E., Kipfstuhl, S., Kjaer, H. A., Koutnik, M., Kuramoto, T., Kohler, P., Laepple, T., Landais, A., Langen, P. L., Larsen, L. B., Leuenberger, D., Leuenberger, M., Leuschen, C., Li, J., Lipenkov, V., Martinerie, P., Maselli, O. J., Masson-Delmotte, V., McConnell, J. R., Miller, H., Mini, O., Miyamoto, A., Montagnat-Rentier, M., Mulvaney, R., Muscheler, R., Orsi, A. J., Paden, J., Panton, C., Pattyn, F., Petit, J. R., Pol, K., Popp, T., Possnert, G., Prie, F., Prokopiou, M., Quiquet, A., Rasmussen, S. O., Raynaud, D., Ren, J., Reutenauer, C., Ritz, C., Rockmann, T., Rosen, J. L., Rubino, M., Rybak, O., Samyn, D., Sapart, C. J., Schilt, A., Schmidt, A. M. Z., Schwander, J., Schupbach, S., Seierstad, I., Severinghaus, J. P., Sheldon, S., Simonsen, S. B., Sjolte, J., Solgaard, A. M., Sowers, T., Sperlich, P., Steen-Larsen, H. C., Steffen, K., Steffensen, J. P., Steinhage, D., Stocker, T. F., Stowasser, C., Sturevik, A. S., Sturges, W. T., Sveinbjornsdottir, A., Svensson, A., Tison, J. L., Uetake, J., Vallelonga, P., van de Wal, R. S. W., van der Wel, G., Vaughn, B. H., Vinther, B., Waddington, E., Wegner, A., Weikusat, I., White, J. W. C., Wilhelms, F., Winstrup, M., Witrant, E., Wolff, E. W., Xiao, C., Zheng, J., and Community, N.: Eemian interglacial reconstructed from a Greenland folded ice core, Nature, 493, 489-494, 10.1038/nature11789, 2013.

de Boer, B., Stocchi, P., and van de Wal, R. S. W.: A fully coupled 3-D ice-sheet-sea-level model: algorithm and applications, Geoscientific Model Development, 7, 2141-2156, 10.5194/gmd-7-2141-2014, 2014.

Dutton, A., Carlson, A. E., Long, A. J., Milne, G. A., Clark, P. U., DeConto, R., Horton, B. P., Rahmstorf, S., and Raymo, M. E.: Sea-level rise due to polar ice-sheet mass loss during past warm periods, Science, 349, 10, 10.1126/science.aaa4019, 2015.

Dyke, L. M., Hughes, A. L. C., Murray, T., Hiemstra, J. F., Andresen, C. S., and Rodés, Á.: Evidence for the asynchronous retreat of large outlet glaciers in southeast Greenland at the end of the last glaciation, Quaternary Science Reviews, 99, 244-259, http://dx.doi.org/10.1016/j.quascirev.2014.06.001, 2014.

Evans, J., Dowdeswell, J. A., Grobe, H., Niessen, F., Stein, R., Hubberten, H. W., and Whittington, R. J.: Late Quaternary sedimentation in Kejser Franz Joseph Fjord and the continental margin of East Greenland, Geological Society, London, Special Publications, 203, 149-179, 2002.

Evans, J., Cofaigh, C. O., Dowdeswell, J. A., and Wadhams, P.: Marine geophysical evidence for former expansion and flow of the Greenland Ice Sheet across the north-east Greenland continental shelf, Journal of Quaternary Science, 24, 279-293, 10.1002/jqs.1231, 2009.

Farrell, W. E., and Clark, J. A.: Post Glacial Sea-Level, Geophysical Journal of the Royal Astronomical Society, 46, 647-667, 1976.

Fyke, J. G., Weaver, A. J., Pollard, D., Eby, M., Carter, L., and Mackintosh, A.: A new coupled ice sheet/climate model: description and sensitivity to model physics under Eemian, Last Glacial Maximum, late Holocene and modern climate conditions, Geoscientific Model Development, 4, 117-136, 10.5194/gmd-4-117-2011, 2011.

Gomez, N., Mitrovica, J. X., Huybers, P., and Clark, P. U.: Sea level as a stabilizing factor for marine-ice-sheet grounding lines, Nature Geosci, 3, 850-853, http://www.nature.com/ngeo/journal/v3/n12/abs/ngeo1012.html - supplementary-information, 2010.

Graversen, R. G., Drijfhout, S., Hazeleger, W., van de Wal, R., Bintanja, R., and Helsen, M.: Greenland's contribution to global sea-level rise by the end of the 21st century, Climate Dynamics, 37, 1427-1442, 10.1007/s00382-010-0918-8, 2011.

Greve, R., Wyrwoll, K. H., and Eisenhauer, A.: Deglaciation of the Northern Hemisphere at the onset of the Eemian and Holocene, Annals of Glaciology, Vol 28, 28, 1-8, 10.3189/172756499781821643, 1999.

Helsen, M. M., van de Wal, R. S. W., van den Broeke, M. R., van de Berg, W. J., and Oerlemans, J.: Coupling of climate models and ice sheet models by surface mass balance gradients: application to the Greenland Ice Sheet, Cryosphere, 6, 255-272, 10.5194/tc-6-255-2012, 2012.

Helsen, M. M., van de Berg, W. J., van de Wal, R. S. W., van den Broeke, M. R., and Oerlemans, J.: Coupled regional climate-ice-sheet simulation shows limited Greenland ice loss during the Eemian, Climate of the Past, 9, 1773-1788, 10.5194/cp-9-1773-2013, 2013.

Hogan, K. A., Cofaigh, C. Ó., Jennings, A. E., Dowdeswell, J. A., and Hiemstra, J. F.: Deglaciation of a major palaeo-ice stream in Disko Trough, West Greenland, Quaternary Science Reviews, http://dx.doi.org/10.1016/j.quascirev.2016.01.018, 2016.

Hutter, K.: Theoretical Glaciology: Material Science of Ice and the Mechanics of Glaciers and Ice Sheets, Springer, 1983.

Huybrechts, P.: Sea-level changes at the LGM from ice-dynamic reconstructions of the Greenland and Antarctic ice sheets during the glacial cycles, Quaternary Science Reviews, 21, 203-231, 10.1016/s0277-3791(01)00082-8, 2002.

Jennings, A. E., Hald, M., Smith, M., and Andrews, J. T.: Freshwater forcing from the Greenland Ice Sheet during the Younger Dryas: evidence from southeastern Greenland shelf cores, Quaternary Science Reviews, 25, 282-298, 10.1016/j.quascirev.2005.04.006, 2006.

Jennings, A. E., Sheldon, C., Cronin, T. M., Francus, P., Stoner, J., and Andrews, J.: The Holocene history of the Nares Strait: Transition from Glacial Bay to Arctic-Atlantic Throughflow, Oceanography, 24, 26-41, 2011.

Jennings, A. E., Walton, M. E., Cofaigh, C. O., Kilfeather, A., Andrews, J. T., Ortiz, J. D., De Vernal, A., and Dowdeswell, J. A.: Paleoenvironments during Younger Dryas-Early Holocene retreat of the Greenland Ice Sheet from outer Disko Trough, central west Greenland, Journal of Quaternary Science, 29, 27-40, 10.1002/jqs.2652, 2014.

Kendall, R. A., Mitrovica, J. X., and Milne, G. A.: On post-glacial sea level - II. Numerical formulation and comparative results on spherically symmetric models, Geophysical Journal International, 161, 679-706, 10.1111/j.1365-246X.2005.02553.x, 2005.

Kopp, R. E., Hay, C. C., Little, C. M., and Mitrovica, J. X.: Geographic Variability of Sea-Level Change, Current Climate Change Reports, 1, 192-204, 10.1007/s40641-015-0015-5, 2015.

Le Meur, E., and Huybrechts, P.: A comparison of different ways of dealing with isostasy: examples from modelling the Antarctic ice sheet during the last glacial cycle", Annals of Glaciology, 23, 1996.

Lecavalier, B. S., Milne, G. A., Simpson, M. J. R., Wake, L., Huybrechts, P., Tarasov, L., Kjeldsen, K. K., Funder, S., Long, A. J., Woodroffe, S., Dyke, A. S., and Larsen, N. K.: A model of Greenland ice sheet deglaciation constrained by observations of relative sea level and ice extent, Quaternary Science Reviews, 102, 54-84, 10.1016/j.quascirev.2014.07.018, 2014.

Letreguilly, A., Reeh, N., and Huybrechts, P.: The Greenland ice-sheet through the last glacial interglacial cycle Global and Planetary Change, 90, 385-394, 1991.

Lisiecki, L. E., and Raymo, M. E.: A Pliocene-Pleistocene stack of 57 globally distributed benthic delta O-18 records, Paleoceanography, 20, 17, 10.1029/2004pa001071, 2005.

Macayeal, D. R.: Large-scale ice flow over a viscous basal sediment - Theory and application to ice stream-B, Antarctica. , Journal of Geophysical Research-Solid Earth and Planets, 94, 4071-4087, 10.1029/JB094iB04p04071, 1989.

Milne, G. A., and Mitrovica, J. X.: Postglacial sea-level change on a rotating Earth, Geophysical Journal International, 133, 1-19, 10.1046/j.1365-246X.1998.1331455.x, 1998.

Mitrovica, J. X., Milne, G. A., and Davis, J. L.: Glacial isostatic adjustment on a rotating earth, Geophysical Journal International, 147, 562-578, 10.1046/j.1365-246x.2001.01550.x, 2001.

Mitrovica, J. X., and Milne, G. A.: On post-glacial sea level: I. General theory, Geophysical Journal International, 154, 253-267, 10.1046/j.1365-246X.2003.01942.x, 2003.

Mitrovica, J. X., Wahr, J., Matsuyama, I., and Paulson, A.: The rotational stability of an ice-age earth, Geophysical Journal International, 161, 491-506, 10.1111/j.1365-246X.2005.02609.x, 2005.

Nowicki, S., Bindschadler, R. A., Abe-Ouchi, A., Aschwanden, A., Bueler, E., Choi, H., Fastook, J., Granzow, G., Greve, R., Gutowski, G., Herzfeld, U., Jackson, C., Johnson, J., Khroulev, C., Larour, E., Levermann, A., Lipscomb, W. H., Martin, M. A., Morlighem, M., Parizek, B. R., Pollard, D., Price, S. F., Ren, D. D., Rignot, E., Saito, F., Sato, T., Seddik, H., Seroussi, H., Takahashi, K., Walker, R., and Wang, W. L.: Insights into spatial sensitivities of ice mass response to environmental change from the SeaRISE ice sheet modeling project II: Greenland, Journal of Geophysical Research-Earth Surface, 118, 1025-1044, 10.1002/jgrf.20076, 2013.

Peltier, W. R.: Impulse response of a maxwell Earth, Reviews of Geophysics, 12, 649-669, 10.1029/RG012i004p00649, 1974.

Peltier, W. R.: Global glacial isostasy and the surface of the ice-age earth: The ice-5G (VM2) model and grace, Annual Review of Earth and Planetary Sciences, 32, 111-149, 10.1146/annurev.earth.32.082503.144359, 2004.

Quiquet, A., Ritz, C., Punge, H. J., and Melia, D. S. Y.: Greenland ice sheet contribution to sea level rise during the last interglacial period: a modelling study driven and constrained by ice core data, Climate of the Past, 9, 353-366, 10.5194/cp-9-353-2013, 2013.

Reerink, T. J., Kliphuis, M. A., and van de Wal, R. S. W.: Mapping technique of climate fields between GCM's and ice models, Geosci. Model Dev., 3, 13-41, 10.5194/gmd-3-13-2010, 2010.

Reerink, T. J., van de Berg, W. J., and van de Wal, R. S. W.: OBLIMAP 2.0: a fast climate model–ice sheet model coupler including online embeddable mapping routines, Geosci. Model Dev., 9, 4111-4132, 10.5194/gmd-9-4111-2016, 2016.

Ritz, C., Fabre, A., and Letreguilly, A.: Sensitivity of a Greenland ice sheet model to ice flow and ablation parameters: Consequences for the evolution through the last climatic cycle, Climate Dynamics, 13, 11-24, 10.1007/s003820050149, 1996.

Ritz, C., Rommelaere, V., and Dumas, C.: Modeling the evolution of Antarctic ice sheet over the last 420,000 years: Implications for altitude changes in the Vostok region, Journal of Geophysical Research-Atmospheres, 106, 31943-31964, 10.1029/2001jd900232, 2001.

Robinson, A., Calov, R., and Ganopolski, A.: Greenland ice sheet model parameters constrained using simulations of the Eemian Interglacial, Climate of the Past, 7, 381-396, 10.5194/cp-7-381-2011, 2011.

Rovere, A., Stocchi, P., and Vacchi, M.: Eustatic and Relative Sea Level Changes, Current Climate Change Reports, 2, 221-231, 10.1007/s40641-016-0045-7, 2016.

Sheldon, C., Jennings, A., Andrews, J. T., Cofaigh, C. O., Hogan, K., Dowdeswell, J. A., and Seidenkrantz, M. S.: Ice stream retreat following the LGM and onset of the west Greenland current in Uummannaq Trough, west Greenland, Quaternary Science Reviews, 147, 27-46, 10.1016/j.quascirev.2016.01.019, 2016.

Simpson, M. J. R., Milne, G. A., Huybrechts, P., and Long, A. J.: Calibrating a glaciological model of the Greenland ice sheet from the Last Glacial Maximum to present-day using field observations of relative sea level and ice extent, Quaternary Science Reviews, 28, 1631-1657, 10.1016/j.quascirev.2009.03.004, 2009.

Stone, E. J., Lunt, D. J., Annan, J. D., and Hargreaves, J. C.: Quantification of the Greenland ice sheet contribution to Last Interglacial sea level rise, Climate of the Past, 9, 621-639, 10.5194/cp-9-621-2013, 2013.

van Angelen, J. H., van den Broeke, M. R., Wouters, B., and Lenaerts, J. T. M.: Contemporary (1960–2012) Evolution of the Climate and Surface Mass Balance of the Greenland Ice Sheet, Surveys in Geophysics, 35, 1155-1174, 10.1007/s10712-013-9261-z, 2014.

van de Wal, R. S. W.: Processes of buildup and retreat of the Greenland Ice Sheet, Journal of Geophysical Research: Atmospheres, 104, 3899-3906, 10.1029/1998JD200030, 1999a.

van de Wal, R. S. W.: The importance of thermodynamics for modeling the volume of the Greenland Ice Sheet, Journal of Geophysical Research: Atmospheres, 104, 3887-3898, 10.1029/1998JD200084, 1999b.

Vasskog, K., Langebroek, P. M., Andrews, J. T., Nilsen, J. E. O., and Nesje, A.: The Greenland Ice Sheet during the last glacial cycle: Current ice loss and contribution to sea-level rise from a palaeoclimatic perspective, Earth-Science Reviews, 150, 45-67, 10.1016/j.earscirev.2015.07.006, 2015.

Winsor, K., Carlson, A. E., Welke, B. M., and Reilly, B.: Early deglacial onset of southwestern Greenland ice-sheet retreat on the continental shelf, Quaternary Science Reviews, 128, 117-126, 10.1016/j.quascirev.2015.10.008, 2015.

Yau, A. M., Bender, M. L., Blunier, T., and Jouzel, J.: Setting a chronology for the basal ice at Dye-3 and GRIP: Implications for the long-term stability of the Greenland Ice Sheet, Earth and Planetary Science Letters, 451, 1-9, 10.1016/j.epsl.2016.06.053, 2016.

Zweck, C., and Huybrechts, P.: Modeling of the northern hemisphere ice sheets during the last glacial cycle and glaciological sensitivity, Journal of Geophysical Research-Atmospheres, 110, 24, 10.1029/2004jd005489, 2005.

Clim. Past Discuss., https://doi.org/10.5194/cp-2017-132
Manuscript under review for journal Clim. Past
Discussion started: 16 October 2017

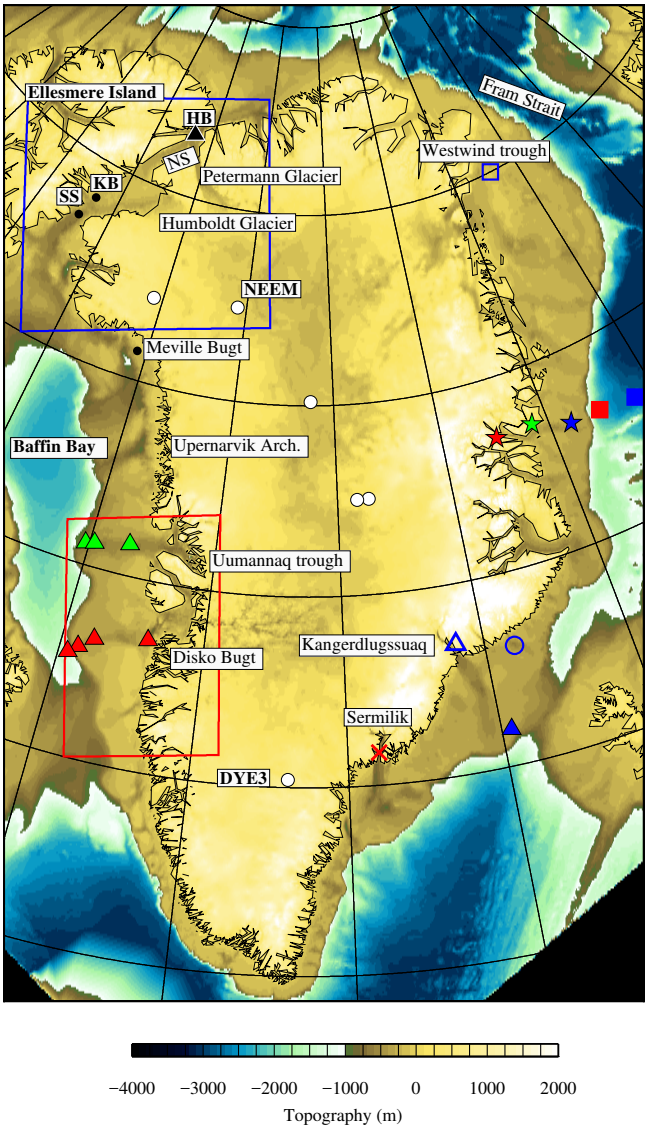

755

Figure 1: Summary of the main places names and regions referred to in the main text and location of observational data. All information describing the symbols and references for the observational data in listed in Table 1. The red and blue boxes highlight the regions shown on Fig.7 and Fig.8 respectively.

Clim. Past Discuss., https://doi.org/10.5194/cp-2017-132
Manuscript under review for journal Clim. Past
Discussion started: 16 October 2017

Climate of the Past Discussions
Open Access
EGU

760

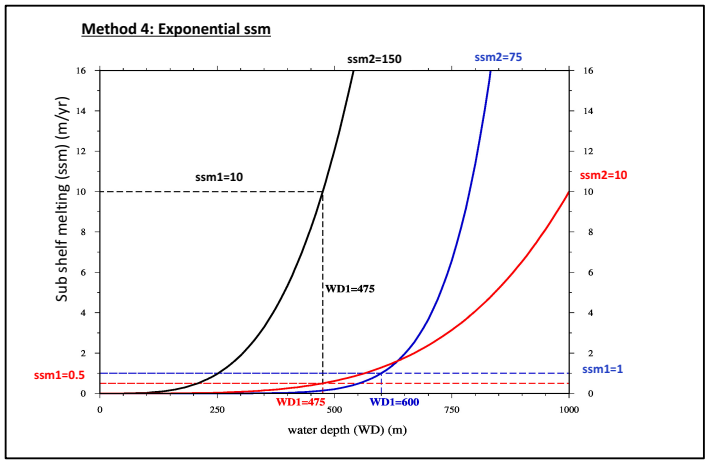

765 **Figure 2: Schematic illustration of the four examples of the SSM parameterisation Method 4: exponential sub-ice shelf melting**

770

775

780

Clim. Past Discuss., https://doi.org/10.5194/cp-2017-132
Manuscript under review for journal Clim. Past
Discussion started: 16 October 2017

Climate of the Past Discussions
Open Access
EGU

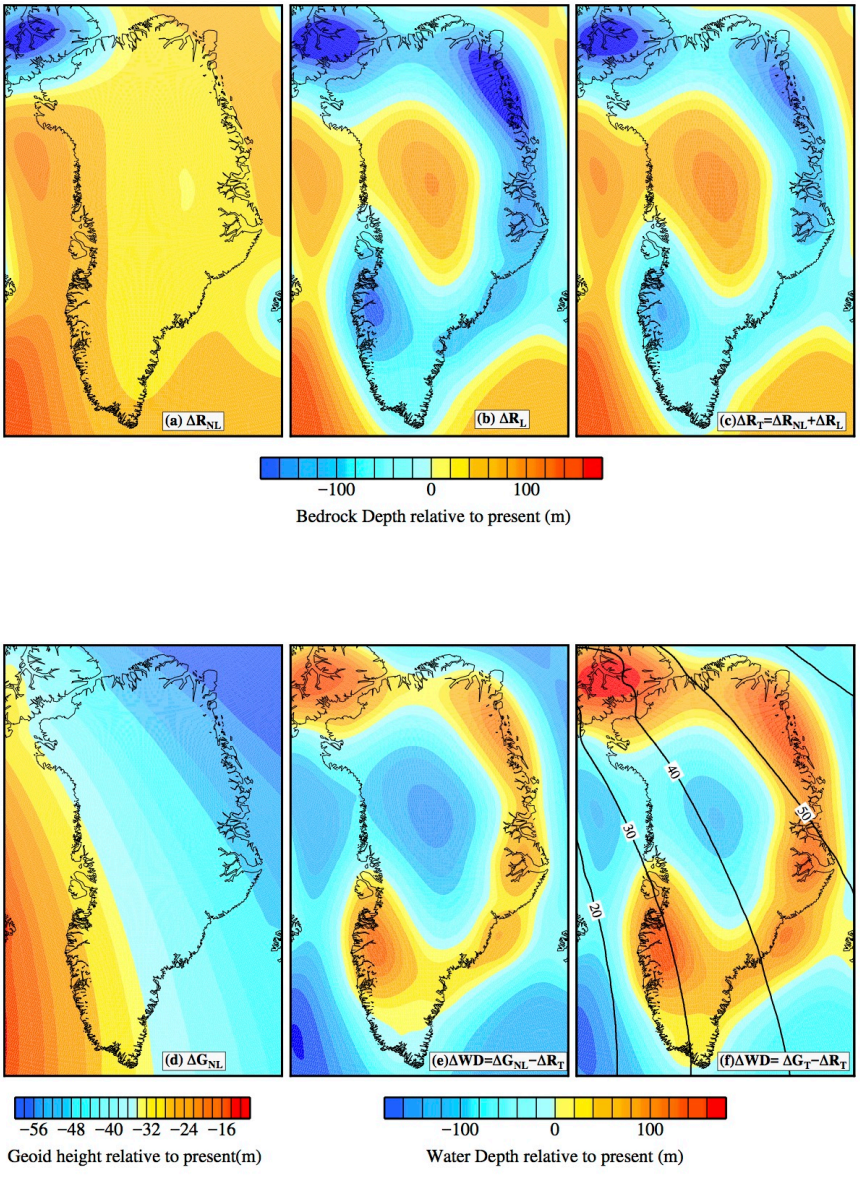

785

Figure 3: Illustration of the various components used within the calculation of the offline RSL forcing at 135 kyr BP. Panels (a-c) are the predicted (solid earth deformation) bedrock depth, ΔR : (a) non-local component, ΔR_{NL} (No GrIS), (b) Local component, ΔR_L (GrIS only) and (c) Total signal, ΔR_T (d) Predicted
790 **non-Local Geoid signal, ΔG_{NL} (No GrIS). The predicted RSL/water depth signal is illustrated for: (e) $\Delta G_{NL} - \Delta R_T$: Combination of Total Predicted bedrock depth and non-local Geoid. It this signal which is used within all simulations. (f) Total water depth signal, ΔWD. Contoured is the local signal, ΔG_L which is not included. See text for extra details.**

Clim. Past Discuss., https://doi.org/10.5194/cp-2017-132
Manuscript under review for journal Clim. Past
Discussion started: 16 October 2017

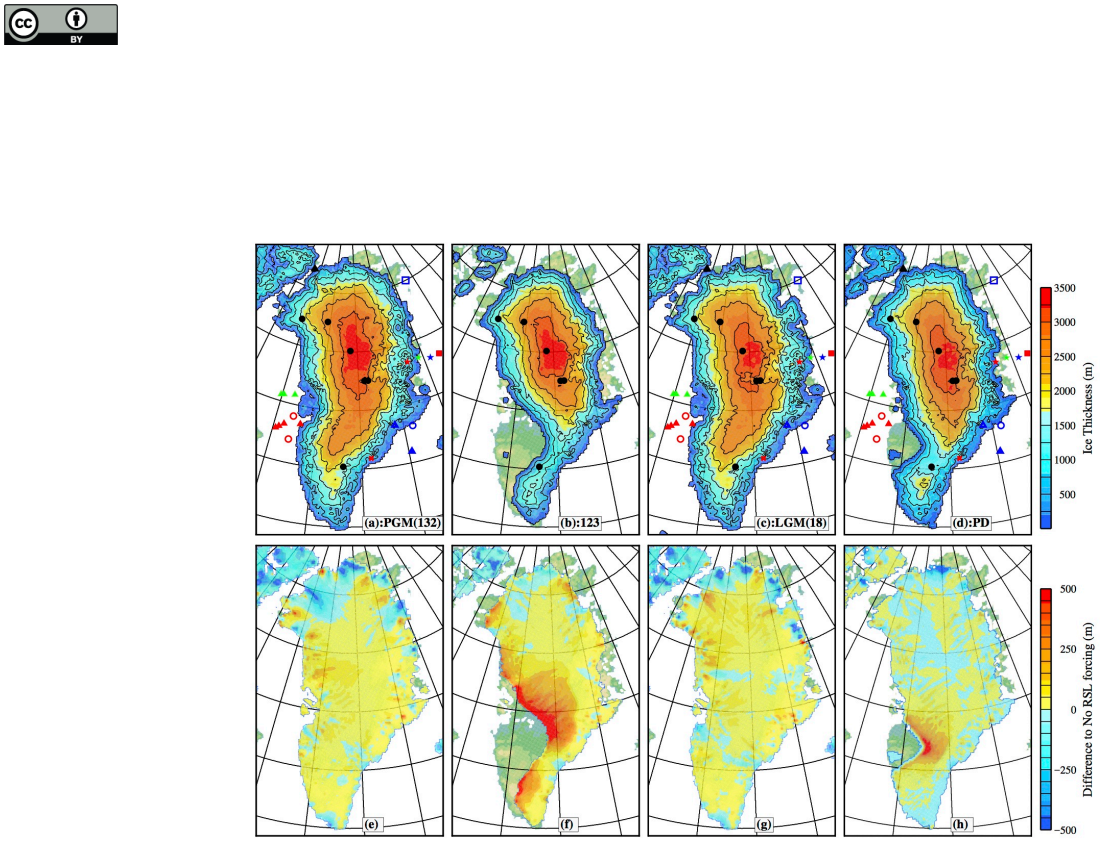

795

Figure 4: Simulated Surface Elevation from simulations using the sheet-only combined with RSL forcing with an As of 1.0 ×10-10 m8N-3yr-1: (a) Penultimate Glacial Maximum (PGM), 132 kyr BP; (b) 123 kyr BP, LIG minimum; (c) Last Glacial Maximum (LGM), 18 kyr BP and (d) Present day (PD). Panels (e), (f), (g) and (h) are the differences relative to the sheet-only simulation using an ESL forcing (no RSL forcing), where a positive thickness indicates a thicker ice sheet with RSL forcing. The black circles mark the location of the GrIS ice core sites. Observed data constraining the timing of retreat are summarised on Table1.

800

805

Clim. Past Discuss., https://doi.org/10.5194/cp-2017-132
Manuscript under review for journal Clim. Past
Discussion started: 16 October 2017

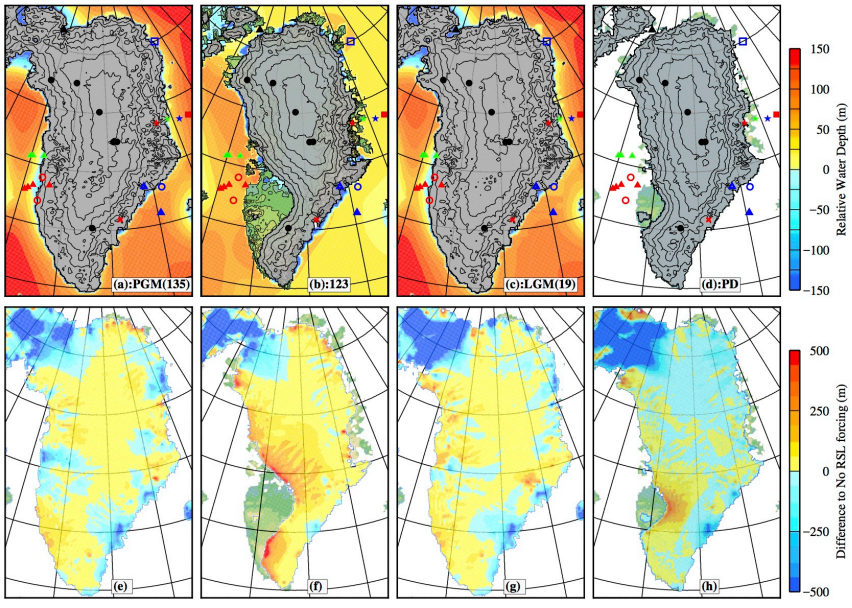

Figure 5: Simulated extent of the grounded ice sheet and relative water depth from simulations using with shelves combined with a RSL forcing and SSM Method4 (AvAs+AvSSM1, parameters highlighted on Table3): (a) Penultimate Glacial Maximum (PGM), 135 kyr BP; (b) 123 kyr BP, LIG minimum; (c) Last Glacial Maximum (LGM), 19 kyr BP and (d) Present day (PD). Panels (e), (f), (g) and (h) are differences relative to the with-shelves simulation using an ESL forcing (no RSL forcing). The black circles mark the location of the GrIS ice core sites. Observed data constraining the timing of retreat is summarised on Table1. Note that the colour bar extended beyond (+/-) 150. Small floating ice shelves formed at the edge of the grounded ice sheet, but these are not shown.

Clim. Past Discuss., https://doi.org/10.5194/cp-2017-132
Manuscript under review for journal Clim. Past
Discussion started: 16 October 2017

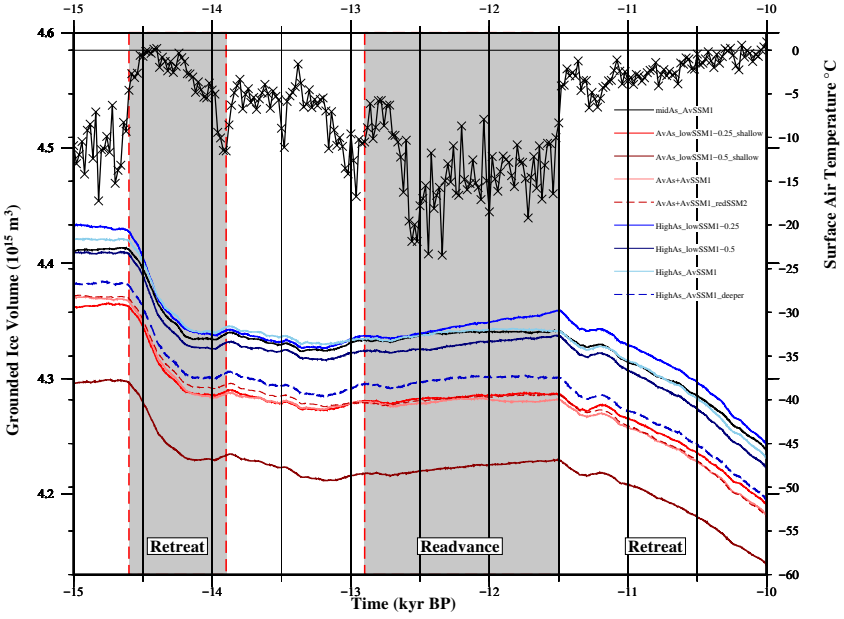

Figure 6: Comparison of the Grounded Ice Volume (10^{15} m^3) from the nine optimum simulations on Table 3 (see Table for colours) and the Surface Air Temperature forcing (°C) (black line with crosses, Fig.S1) from 15 to 10 kyr BP. Highlighted are the timings of the retreat-readvance-retreat of the SW margin (red box, Fig.1), the spatial pattern of which is illustrated for A_vA_s+A_vSSM1 (light red line) on Fig.7. The retreat pattern across the NW is illustrated on Fig.8 for two extreme simulations: A_vA_s_lowSSM1-0.5_shallow (dark red) and HighA_s_lowSSM1-0.25 (blue line).

Clim. Past Discuss., https://doi.org/10.5194/cp-2017-132
Manuscript under review for journal Clim. Past
Discussion started: 16 October 2017

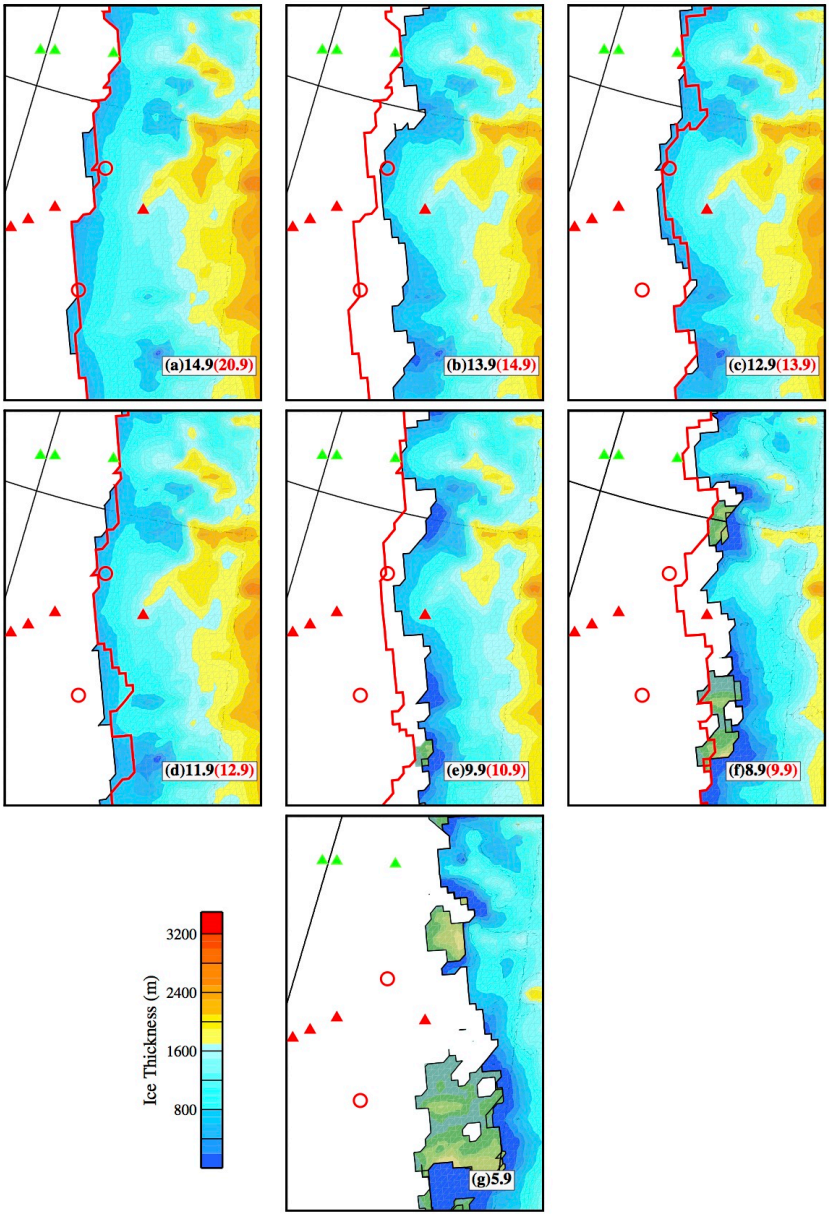

Figure 7: Retreat of the grounded ice sheet along the SW margin (region bounded by the red box on Fig.1) for AvAs+AvSSM1 (kyr BP). The red contour marks the edge of the grounded ice sheet at an earlier time step (given in red): (a) 14.9 (20.9); (b) 13.9 (14.9); (c) 12.9 (13.9); 11.9 (12.9); (e) 9.9 (10.9) (f) 8.9 (9.9) and (g) 5.9. There is minimal change between the extent at 5.9 and present day. Observed data constraining the timing of retreat are summarised on Table1. Small floating ice shelves formed at the edge of the grounded ice sheet, but these are not shown.

Clim. Past Discuss., https://doi.org/10.5194/cp-2017-132
Manuscript under review for journal Clim. Past
Discussion started: 16 October 2017

Climate of the Past Discussions
Open Access
EGU

835

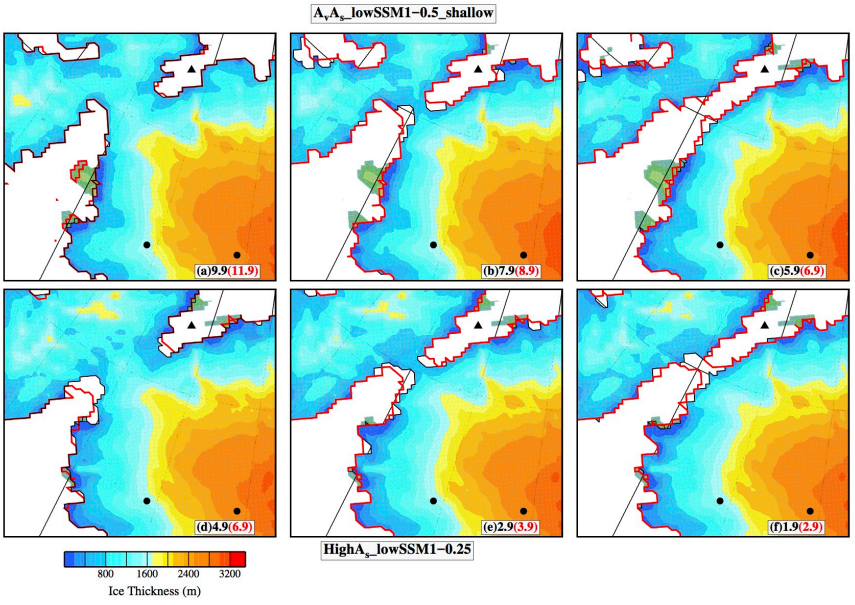

840 **Figure 8: Retreat of the grounded ice sheet across the Nares Strait, NW margin (region bounded by the blue box on Fig.1) for two contrasting simulations (in kyr BP), the red contour marks the edge of the grounded ice sheet at an earlier time step (given in red). AvAs_lowSSM1-0.5_shallow (a) 9.9 (11.9); (b) 7.9 (8.9) and (c) 5.9 (6.9) and HighAs_lowSSM1-0.25 (d) 4.9 (6.9); (e) 2.9 (3.9) and (f) 1.9 (2.9). For panels (c) and (f) there is minimal change between the extent at this time step and the extent at present day. Observed data**
845 **constraining the timing of retreat are summarised on Table1. Small floating ice shelves formed at the edge of the grounded ice sheet, but these are not shown.**

850

Clim. Past Discuss., https://doi.org/10.5194/cp-2017-132
Manuscript under review for journal Clim. Past
Discussion started: 16 October 2017

Climate of the Past Discussions
Open Access
EGU

Symbol	Name	Region	Location and Material	Latitude	Longitude	Timing deglaciation	Reference
▲	HLY03-01-05GC	North West	Core -Hall Basin	81.62° N	296.74° W	< 9 kyr BP	Jennings et al., 2011
▭	Swath bathymetry & TOPAS acoustic data	North East	Near Westwind Trough	~ 80° N	~ 346 °W	Evidence for grounded ice	Evans et al., 2009
★	Kejser Franz	Central East	Core- Inner shelf Moraine	73.45° N	335° W	before 7.4 kyr BP	Evans et al., 2002
★	Fosters Bugt	Central East	Core- Mid shelf Moraine	73.5°N	338.5° W	stablised ~ 10 kyr BP	Evans et al., 2002
★	PS2630	Central East	Core - Outer shelf	73.15° N	341.9° W	< 15 kyr BP	Evans et al., 2002
■	PS2628	Central East	Cores - NE Greenland Basin	73.15° N	344.75° W	~ 13 kyr BP	O'Cofaigh et al., 2004
■	GC25	Central East	Cores - NE Greenland Basin	73.01° N	348.13° W	~ 13 kyr BP	O'Cofaigh et al., 2004
○	MD99-2371	South East	Core - Grivel Basin Denmark Strait	68.09° N	332.06° W	14.3-13.8 kyr BP	Jennings et al., 2006
▲	Core	South East	Outer Kangerdlugssuaq Trough	65.96° N	330.63° W	17.2 kyr BP	Dyke et al., 2004
△	MD99-2371	South East	Inner Kangerdlugssuaq Fjord	68.43° N	328.06° W	11.8 kyr BP	Dyke et al., 2004
X	MD99-2371	South East	Inner Sermilik Fjord	65.86° N	322° W	10.9 kyr BP	Dyke et al., 2004
▲	VC15	South West	Core - Disko Trough	67.91° N	301.27° W	~ 12.24 kyr BP	Hogan et al., 2016
▲	VC35	South West	Core - Disko Trough	67.70° N	300.66° W	12.35	Jennings et al., 2014
▲	VC20	South West	Core - Disko Trough	68.20° N	302.24° W	12.2	Jennings et al., 2014
▲	MSM343300	South West	Core - Disko Bugt	68.47° N	306.0° W	10.9	Hogan et al., 2106
○	Hellefiske	South West	moraine - approx.central	~ 67.0° N	~ 304° W	Evidence for	Hogan et al., 2016
	moraine		location	~ 69.0° N	~ 304° W	grounded ice	Hogan et al., 2016
▲	JR175-VC45	Central West	Core - Uummannaq trough	70.56° N	299.63° W	> 14.9 kyr BP	Sheldon et al., 2016
▲	JR175- VC43	Central West	Core - Uummannaq trough	70.62° N	300.38° W	11.4 kyr BP	Sheldon et al., 2016
▲	MSM343520	Central West	Core - Uummannaq trough	70.82 N	303.152 W	< 10.8 kyr BP	Sheldon et al., 2016

Table 1: Summary of a selection of the observational data which were used to constraint the timing and spatial extent of the grounded ice sheet.

Parameter	Method 1 Constant SSM	Method 2 Stepped SSM	Method 3 Exponential + Constant	Method 4 Exponential
A_s (m^{-8} N^3 yr^{-1})	1.0×10^{-10}	0.1 & 1.0×10^{-10}	0.1×10^{-10}	0.04 - 1.2×10^{-10}
SSM1 (m/yr)	0.25 - 10	0.25	0.25 - 1.5	0.25 - 10
SSM2 (m/yr)	–	2.45	2.45; 5; 10	10 - 150
water depth1 (m)	–	450, 600, 800	475-700	300 - 600
water depth 2 (m)	–	–	–	1000

Table 2: Range of parameters adopted in the four sub-ice shelf melting (SSM) parameterisations, illustrated on Fig. S2. Method 4 is also shown in greater detail on Fig.2.

Clim. Past Discuss., https://doi.org/10.5194/cp-2017-132
Manuscript under review for journal Clim. Past
Discussion started: 16 October 2017

Climate of the Past Discussions
Open Access
EGU

Abbreviated Name	Colour Fig 6	A× 10^{-15} ($m^n N^{-3} yr^{-1}$)	SSM1 (m/yr)	WD 1 (m)	SSM2 (m/yr)	Timing -NW (kyr BP) PGM - LIG	LGM - PD	TOTAL LIG ESL(m)/ (Ice Volume *10^{15} m^3) shelf+RSL	Diff to ESL	sheet only	Diff to sheet only	LGM ESL (m) shelf+RSL	Diff to ESL	sheet only	Diff to sheet only
LowA_lowSSM1-0.25_deep	-	0.1	0.25	550	150	NONE	3.9 - 2.9	1.62 (2.97)	*0.45*	0.97 (2.72)	*-0.61*	-1.90	*-0.28*	-0.89	*1.01*
midA_AvSSM1	black	0.8	1	400	100	129.0 - 128.0	0.9 - 0	1.55 (2.75)	*-0.16*	1.02 (2.51)	*-0.58*	-2.52	*-0.17*	-1.30	*1.22*
AvA_lowSSM1-0.25_shallow	red	1	0.25	300	150	129.0 - 127.9	3.9 - 2.9	1.44 (2.73)	*0.30*	1.06 (2.37)	*-0.88*	-2.57	*-0.27*	-1.34	*1.23*
AvA_lowSSM1-0.5_shallow	dark red	1	0.5	300	150	129.0 - 127.9	7.9 - 6.9	1.36 (2.76)	*-0.22*	1.06 (2.37)	*-0.95*	-2.47	*-0.32*	-1.34	*1.13*
AvA+AvSSM1	light red	1	1	400	100	129.0 -127.9	6.9 - 5.9	1.42 (2.72)	*-0.08*	1.06 (2.37)	*-0.85*	-2.61	*-0.12*	-1.34	*1.27*
AvA+AvSSM1_redSSM2	dashed red	1	1	400	75	128.9 - 128.0	8.9 - 7.9	1.50 (2.71)	*0.50*	1.06 (2.37)	*-0.83*	-2.58	*-0.48*	-1.34	*1.24*
HighA_lowSSM1-0.25	blue	1.2	0.25	475	150	128.0 - 126.9	2.9 - 1.9	1.25(2.68)	*0.50*	1.12 (2.39)	*-0.92*	-2.87	*-0.33*	-1.42	*1.45*
HighA_lowSSM1-0.5	dark blue	1.2	0.5	475	150	127.9 - 126.9	1.9 - 0.9	1.45 (2.73)	*0.49*	1.12 (2.39)	*-0.70*	-2.83	*-0.36*	-1.42	*1.41*
HighA_AvSSM1	light blue	1.2	1	400	100	129.0 - 127.9	1.9 - 0.9	1.50 (2.73)	*0.33*	1.12 (2.39)	*-0.83*	-2.81	*-0.14*	-1.42	*1.39*
HighA_AvSSM1_deeper	dashed blue	1.2	1	475	150	127.9 - 126.9	1.9 - 0.9	1.49 (2.68)	*0.38*	1.12 (2.39)	*-0.70*	-2.71	*-0.39*	-1.42	*1.29*
HighA_highSSM1	--	1.2	5	475	150	NONE	6.9 - 5.9	1.48 (2.64)	*-0.14*	1.12 (2.39)	*-0.61*	-2.59	*-0.25*	-1.42	*1.17*

Table 3: Set of optimum parameters using SSM Method 4, with shelves and RSL forcing, which resulted in a growth beyond the present-day margin during glacial maximums (PGM and LGM) and a retreat by present day. Note that WD2 is constant in all simulations, 1000m. The simulation highlighted in grey is shown on Fig.5. The timing of the retreat across the Nares Strait for two interglacial is given (Timing-NW (kyr BP)): PGM-LIG and LGM-PD. The total ice-volume equivalent sea-level (ESL) contribution from the GrIS only for the Last interglacial (LIG) and the Last Glacial Maximum (LGM) from with shelves and RSL forcing, and sheet-only (ESL forcing) simulation is listed, with the differences calculated relative to with shelves and ESL forcing (Diff to ESL) and relative to sheet-only (Diff to sheet-only). To calculate the relative difference (shown in italics) in the ESL contribution for the LIG interval (between with shelves and ESL forcing and sheet-only simulations), the difference in the LIG ice volume (given in brackets) was used. For the LGM, the difference in the total ESL contribution was used, where a positive difference indicates an increase in the GrIS contribution: a negative a reduction.